Hardware and Control Implementation of Electric Springs for Stabilizing Future Smart Grid With Intermittent Renewable Energy Sources

Chi Kwan Lee, *Member, IEEE*, Balarko Chaudhuri, *Senior Member, IEEE*, and Shu Yuen Hui, *Fellow, IEEE*

***Abstract*— In this paper, the details of practical circuit and control implementation of an electric spring for reactive power compensation and voltage regulation of the ac mains are presented. With Hooke's law published three centuries ago, power electronics-based reactive power controllers are turned into electric springs (ESs) for regulating the ac mains of a power grid. The proposed ES has inherent advantages of: 1) ensuring dynamic load demand to follow intermittent power generation; and 2) being able to regulate the voltage in the distribution network of the power grid where numerous small-scale intermittent renewable power sources are connected. Therefore, it offers a solution to solve the voltage fluctuation problems for future power grids with substantial penetration of intermittent renewable energy sources without relying on information and communication technology. The proof-of-concept hardware is successfully built and demonstrated in a 10-kVA power system fed by wind energy for improving power system stability. The ES is found to be effective in supporting the mains voltage, despite the fluctuations caused by the intermittent nature of wind power.**

***Index Terms*— Inverter, power smoothing, renewable energy sources, smart grids.**

I. Introduction

With many countries setting new legislations to decarbonize power generation by 20% by 2020 [1]–[3], the use of renewable energy generation has become a global research and development topic. The imminent increase in intermittent and distributed renewable power sources, known or unknown to the utility companies, has raised concerns about the stability of future power grid with substantial renewable power generation. In existing power systems, power is generated by the power companies in a centralized manner to meet the load demand, that is, power generation follows the load demand. For future smart grids with heavy penetration of intermittent and distributed renewable power sources, the new requirement of control paradigm will be for the load demand to follow power generation [4], [5]. This new requirement has triggered new research into modern demand-side management.

So far, recent research activities focused on several demand-side management approaches to fulfill the new control paradigm. Literature review for the period of 2005–2012 showed that demand-side management (or sometimes known as demand response) [6] can be broadly summarized as follows:

1) scheduling of delay-tolerant power demand tasks [7]–[9];
2) use of energy storage to alleviate peak demands [10];
3) real-time pricing [11]–[13];
4) direct load control or on−off control of smart loads [14]–[16].

Although these methods have their own advantages, they also suffer certain inherent limitations. Scheduling of load demand can be done in terms of days or hours, but such method cannot cope with real-time power fluctuation. Energy storage is an ideal solution, but it is either expensive (such as battery) or not geographically available (such as water reservoirs). Real-time pricing can play a certain role and is effective for some price-conscious large customers, but it may not be applicable to ordinary domestic consumers. Traditionally, power companies use direct load control to shed power loads for avoiding power system collapse, but such central control may not be effective for future power grid with substantial decentralized and intermittent renewable energy sources at the distribution networks. On−Off control of electric loads such as water heaters and air conditioners has been proposed, but such approach could be intrusive and cause inconvenience to the consumers. Recent research based on wide-area measurements for feeding information to a data center for central and regional controls has been examined. Data transfer is usually based on information and communication technology (ITC), such as wireless communications, satellite synchronization, and internet/intranet control. This approach should be effective under normal operating conditions, but may be paralyzed when the wireless communications systems are disabled in extreme weather or atmospheric conditions (such as strong solar storms) and/or when the internet is hacked.

In this paper, a new approach to demand-side management based on the electric spring (ES) concept is described. ESs are reactive power controllers [17], [25] that can be embedded in noncritical loads such as electric water heaters,

Manuscript received February 25, 2013; accepted April 25, 2013. Date of publication May 16, 2013; date of current version July 3, 2013. This work was supported in part by the HK Research Grant Council under the Collaborative Research Fund HKU10/CRF/10, and the University of Hong Kong Seed Funding Programme for Basic Research under Grants 201203159010 Grant 201111159239. Recommended for publication by Associate Editor J. Olorunfemi Ojo.

C. K. Lee is with the Department of Electrical and Electronic Engineering, University of Hong Kong, Pokfulam, Hong Kong (e-mail: cklee@eee.hku.hk).

B. Chaudhuri is with the Department of Electrical and Electronic Engineering, Imperial College London, London SW7 2BT, U.K. (e-mail: b.chaudhuri@imperial.ac.uk).

S. Y. Hui is with the Department of Electrical & Electronic Engineering, University of Hong Kong, Pokfulam, Hong Kong, China, and also with Imperial College London, London SW7 2AZ, U.K. (e-mail: ronhui@eee.hku.hk; r.hui@imperial.ac.uk).

Color versions of one or more of the figures in this paper are available online at http://ieeexplore.ieee.org.

Digital Object Identifier 10.1109/JESTPE.2013.2264091

air conditioners, and lighting systems and turned them into a new form of smart loads. They provide reactive power compensation for voltage regulation of ac mains of the power grid. Because of the distributed nature of installations, they provide local voltage support over the distribution network of the power grid. They have an inherent advantageous feature that they can ensure the load demand to automatically follow the power generation profile in real time, without reliance on ICT, smart metering or wide-area measurements. The original concept was described in [25]. Subsequent research led to the theoretical framework of the ES concept, which had the potential to control both active and reactive power [26] and reduce energy storage requirements in a power grid [27]. This is the first paper that covers the detailed practical hardware design and control implementation of an ES for voltage regulation of distribution line. It is tested in a power grid fed by an intermittent wind power profile. Its abilities in stabilizing a fluctuating ac mains and shaping the load demand to follow the wind power profile are demonstrated. The differences among the ESs, static var compensation (SVC) and static synchronous compensator (STATCOM) are also included.

II. Operating Principle of ES

A. From Mechanical Springs to ESs

Hooke's law [18] states that the force of an ideal mechanical spring is as follows:

$$\mathbf{F} = -k\mathbf{x} \tag{1}$$

where $\mathbf{F}$ is the force vector, k is the spring constant, and $\mathbf{x}$ is the displacement vector. The potential energy (PE) stored in the mechanical spring is as follows:

$$\text{PE} = \frac{1}{2}kx^2. \tag{2}$$

Analogous to a mechanical spring, an ES is an electric device that can be used to: 1) provide electric voltage support; 2) store electric energy; and 3) damp electric oscillations. Analogous to (1), the basic physical relationship of the ES is expressed as [25] follows:

$$q = -Cv_a \tag{3}$$

$$q = \int i_c dt \tag{4}$$

where q is the electric charge stored in a capacitor with capacitance C, v_a is the electric potential difference across the capacitor, and i_c is the current flowing into the capacitor. The energy storage capability of the ES can be seen from the potential electric energy stored in the ES is as follows:

$$PE = \frac{1}{2}Cv_a^2. \tag{5}$$

Therefore, the capacitor C serves as the energy storage element for the ES. Equation (4) shows that the charge (q) can be altered using a controlled current source. Therefore, the bouncing action of the ES can be practically realized with the use of power electronics-based reactive power controller. Comparisons of the formats of (1) and (3), and those of (2) and (5) highlight the similarities between the mechanical spring and ESs [25].

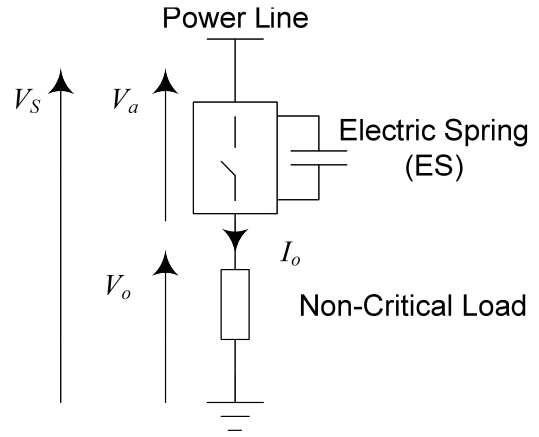

Fig. 1. Simplified connection diagram of an ES.

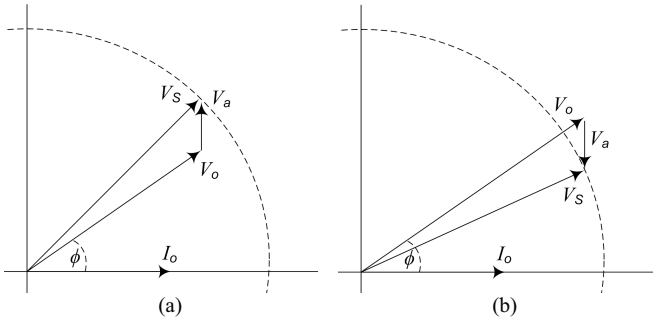

Fig. 2. Vectors diagrams of ES operates under (a) inductive mode and (b) capacitive mode with an inductive load.

B. Operating Principle of ESs

As an ES should provide a function for damping electric oscillations, it is necessary to connect the lossless ES in series with a dissipative electric load (such as a water heating system or a refrigerator or a combination of them). Fig. 1 shows a simplified connection diagram of an ES. The output of the ES is connected to a noncritical load to form a smart load [25]. The noncritical load can be a single or a group of electric loads that can tolerate some degrees of voltage variation without causing significant inconvenience to the user. Examples are electric water heaters and some public lighting systems. For reactive power compensation, the ES only processes the reactive power and the compensation voltage vector V_a is perpendicular to the noncritical load current I_o. The V_a can be controlled either 90° lagging or leading to the I_o Therefore, it generates either inductive or capacitive reactive power to the power system. Unlike traditional FACT devices such as SVC and STATCOM that handle pure reactive power only, the ES is a new smart-grid device that can alter both active and reactive power. Although its structure resembles a static synchronous series compensator (SSSC) [19]–[21], it differentiates itself from a SSSC by the following: 1) employing an input voltage control rather than an output voltage control; and 2) having the ability to alter the active and reactive power in the series-connected noncritical load.

The vectors diagrams of an ES operated under inductive and capacitive modes with an inductive load are shown in Fig. 2. The vectorial sum of the noncritical load voltage V_o

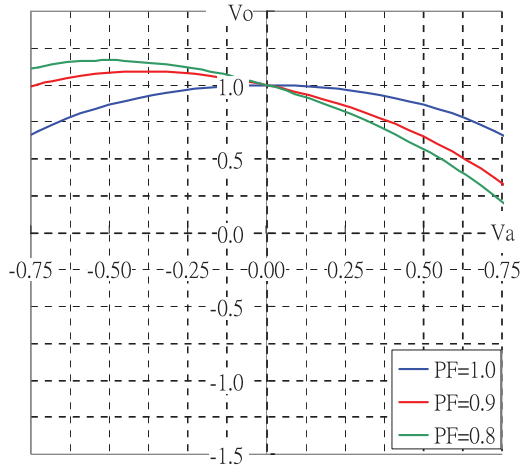

Fig. 3. Normalized noncritical load voltage (V_o) against compensation voltage (V_a) at different load power factors (V_a is normalized to 220 Vac).

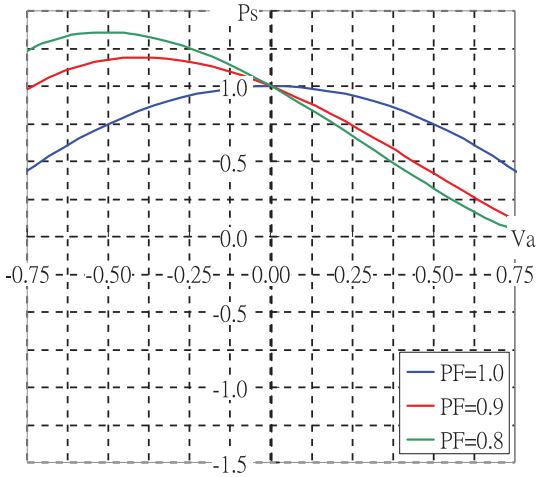

Fig. 4. Normalized smart load power (P_S) against compensation voltage (V_a) at different load power factors (V_a is normalized to 220 Vac).

and the compensation voltage V_a is equal to the supply voltage V_S. With the observation of the vector diagrams, V_o can be boosted or suppressed by V_a which is generated by the ES. Therefore, the power consumption of the noncritical load can be controlled. Mathematically, the mains voltage V_S of the power line and the ES operated under inductive or capacitive mode can be expressed as follows:

$$V_S^2 = (V_o \cos\phi)^2 + (V_o \sin\phi \pm V_a)^2 \tag{6}$$

where ϕ is the power factor angle of the noncritical load. The vector direction of the compensation voltage V_a under the inductive mode [Fig. 2(a)] and the capacitive mode [Fig. 2(b)] is given in (7) as follows:

$$V_a = \begin{cases} +v & \text{inductive mode} \\ -v & \text{capacitive mode.} \end{cases} \tag{7}$$

Solving (6), the noncritical load voltage V_o can be expressed as (8) as follows:

$$V_o = \frac{-2V_a \sin\phi \pm \sqrt{(2V_a \sin\phi)^2 - 4\left(V_a^2 - V_S^2\right)}}{2} = -V_a \sin\phi + \sqrt{V_a^2 \sin^2\phi - V_a^2 + V_S^2} \tag{8}$$

(taking the positive root).

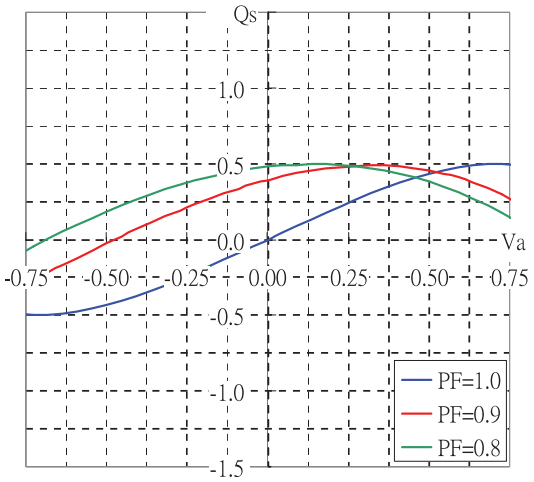

Fig. 5. Normalized smart load reactive power (Q_S) against compensation voltage (V_a) at different load power factors (V_a is normalized to 220 Vac).

The corresponding noncritical load current I_o, active and reactive power (P_S, Q_S) of the entire smart load can be analytically obtained as follows:

$$I_o = \frac{V_o}{Z_1} = \frac{V_o}{\sqrt{R_1^2 + X_1^2}} \tag{9}$$

$$P_S = V_o I_o \cos\phi = \frac{V_o^2 \cos\phi}{Z_1} \tag{10}$$

$$Q_S = V_o I_o \sin\phi + V_a I_o = \frac{V_o^2 \sin\phi + V_o V_a}{Z_1} \tag{11}$$

where Z_1 is the impedance of the noncritical load. The characteristic of the noncritical load V_o (normalized to the rated mains voltage V_S) against the compensation voltage V_a at different power factor angles is plotted in Fig. 3. The active power P_S and reactive power Q_S characteristics normalized to the rated power are plotted in Figs. 4 and 5, respectively. Depending on the power factor of the noncritical load, the ES can, in principle, perform active and/or reactive power controls (which make it fundamentally different from traditional FACT devices such as SVC and STATCOM) [26]. For instance, the change of compensation voltage V_a can simultaneously provides reactive power compensation and load shedding to the power system when the power factor of the noncritical load is close to unity. Generally, the active power consumption can be altered when an ES is connected to a load with nonunity power factor. With the use of input voltage (V_s) control mechanism and letting the noncritical load voltage V_o to fluctuate dynamically, the ES can be a useful apparatus for shaping the load demand to follow the electric power generation. This important feature of an ES can improve the instantaneous power balance, power quality, and stability of the future electric power grid with high penetration of intermittent renewable energy sources in real time.

III. Practical Implementation

A. Power Inverter Circuit

A variety of power inverter topologies such as single-phase, three-phase, and two-level or multilevel inverters [22], [23]

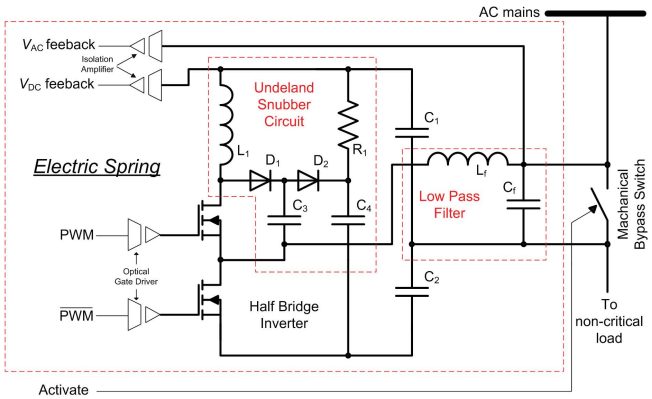

Fig. 6. Schematic of a single-phase half-bridge power inverter.

TABLE I
ES SPECIFICATIONS

Electric Spring Power Circuit	
Inverter Topology:	Single Phase Half Bridge Inverter
Switching Frequency:	20kHz
Regulated DC-Bus Voltage:	400Vdc
DC Bus Capacitance:	C1 = 3000μF, C2 = 3000μF
Inverter Output Voltage Range:	0 ~ 134Vac, Controlled by the Modulation Index (M)
Power MOSFET:	IRFP31N50L
Typical $R_{DS(on)}$:	0.15Ω @ I_D=31A
Output Low Pass Filter:	
Measured Inductance:	500μH@100Hz
Measured Equivalent Series Resistance:	0.09Ω@100Hz
Capacitance:	13.2μF

can be used to implement an ES. Fig. 6 shows the power inverter circuit of an ES that is practically implemented by a single-phase half-bridge power inverter. To observe the performance changes of the power system with and without an ES installation, a mechanical bypass switch is connected across the output terminals during the experiments. A sinusoidal pulsewidth-modulated (PWM) control signal is generated by the control circuit to provide the gating signals for the power inverter. The PWM voltage output of the inverter is filtered by the low-pass *LC* filter hence the compensation voltage is sinusoidal. In a PWM inverter, the power switches could suffer from the high turn-on loss because of the high recovery current generated from the freewheeling diodes and the turn-off snubber capacitors. Thus, a turn-on snubber should be included to overcome the problem. In this ES prototype, an Undeland snubber is used. It includes the turn-off over-voltage and turn-on over-current protections for the power inverter [24]. The turn-off snubber capacitors of the upper and lower switches are combined into a single capacitor. Thus, the power loss of the entire protection circuit is lower than the traditional snubber configuration. The MOSFETs used in the prototype are IRFP31N50L with fast and soft recovery body diode that can reduce the turn-on loss and electromagnetic interference problem. The magnetic core of the output *LC* filter is an iron-based Metglas amorphous alloy. It has the advanced features of low-loss and high-saturation flux density. Therefore, the efficiency and the output harmonic distortion of the ES can be substantially improved. The detail specifications of the power inverter prototype are summarized in Table I.

B. Control Circuit

It is important to note the differences between the proposed ES and other traditional reactive power compensation methods such as SSSC and dynamic voltage restorer. Traditional reactive power compensators: 1) use the output-voltage control for regulating the output voltage of the reactive power converters; and 2) handle reactive power only. ESs: 1) adopt input-power control for regulating the input voltage of the reactive power converters; and 2) provide additional load shedding functions (i.e., real power control) for the noncritical load.

The control of the ES differentiates itself from the traditional SSSC using output-voltage control method. With the input-voltage control mechanism, an ES regulates the mains voltage V_s (which is the input voltage of the reactive power controller) by controlling the power flow to the noncritical load and allows the noncritical load voltage V_o (which is the output voltage of the reactive power controller) to fluctuate dynamically. This means that the output voltage of the ES is not dynamically regulated. The noncritical load power is shaped simultaneously to follow the available power generated by the power system. Therefore, it is a new demand-side management method that can satisfy the new control paradigm of having the load demand following the power generation. A simplified control block diagram of the ES is shown in Fig. 7. The ES requires two closed-loop controllers to operate. With the analysis in Section II, the reactive power is directly controlled by varying the amplitude of the compensation voltage V_a across the filter capacitor of the ES. In this form of implementation, the ES does not process the active power theoretically. Practically, a small amount of active power will be consumed because of the power losses of the power inverter and the *LC* filter. Thus, the dc bus voltage of the power inverter can be regulated. The active power consumption is controlled by adjusting the phase angle between the V_a and noncritical load current I_o. The relationship of phase angle θ (which is the angle between vectors of V_s and V_a) and active power consumption under the inductive and capacitive modes of operation are shown in Fig. 8.

The instantaneous mains voltage v_s is measured by a voltage sensor and sampled by an analog-to-digital converter at 20 kHz. The root-means-square (rms) value is calculated in every 20 ms. The dc bus voltage v_{DC} measurement module is identical. The signals obtained are connected to the proportional-integral (PI) controller. The transfer function of the PI controller in discrete form is expressed as follows:

$$u(t) = u(t-1) + K_P\left[e(t) - e(t-1)\right] + K_p\frac{T_S}{T_i}e(t) \quad (12)$$

where $u(t)$, $u(t-1)$ and $e(t)$, $e(t-1)$ are the transfer function outputs and error inputs of the controller at the present and past samplings, respectively. K_p is the proportional gain constant. T_i and T_s are the integral time constant and sampling time of the controller, respectively. The control algorithm is implemented in a National Instrument embedded controller.

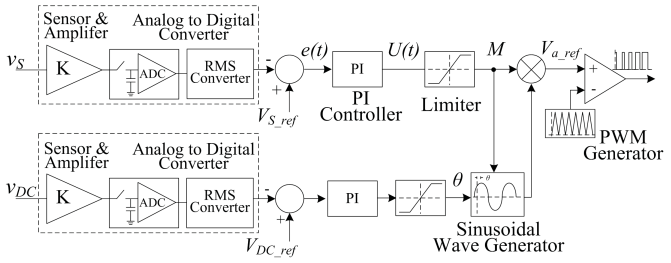

Fig. 7. Simplified control block diagram of an ES for reactive power compensation.

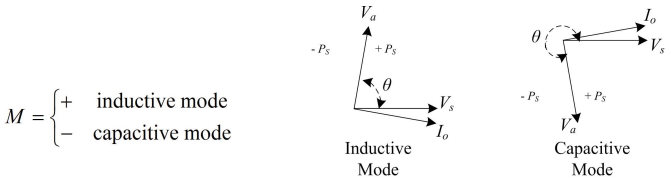

Fig. 8. Relationship of the phase angle and active power consumption.

TABLE II
ES SPECIFICATIONS

NI Embedded Controller			
Switching Scheme:	Sinusoidal PWM		
Minimum to Maximum Modulation Index (M):	0.05 ~ 0.95		
Proportional and Integral Controller	Sampling Time (T_s)	Proportional Gain (K_p)	Integral Gain (K_pK_i/T_s)
AC line voltage:	20ms	30	5
DC bus voltage:	20ms	20	1

The corresponding control parameters are summarized in Table II. The experimental results of the control loop response are recorded in Figs. 11–14.

IV. EXPERIMENTAL SETUP

Fig. 9(a) shows a photograph of the smart-grid experimental setup in the Maurice Hancock Smart Energy Laboratory at Imperial College London. The photograph of the ES prototype and the controller is shown in Fig. 9(b). The experimental setup for evaluating the response of the ES under a weakly regulated power grid is shown in Fig. 10. A 90-kVA power inverter controlled by a digital signal processor is used to emulate a traditional electric power substation. The electric energy is transferred through the distribution network to a remote location, which is represented by the noncritical and critical load resistors. As an example, half of the loads in the remote location are equipped with ESs. A 10-kVA power inverter is used to emulate an intermittent renewable energy source. With the use of the instantaneous $P - Q$ theory, the output active and reactive power (P_R, Q_R) of the renewable energy source can be controlled to inject or absorb active and reactive power. Therefore, the power line voltage V_S is fluctuating around the nominal mains voltage value of 220 Vac because of the intermittent nature of the wind power. The detailed specifications of the power grid are summarized in Table III. A computer-based measurement and data acquisition system is developed to record the instantaneous voltage and current at different nodes of the power grid for recording the information of the active and reactive power flows.

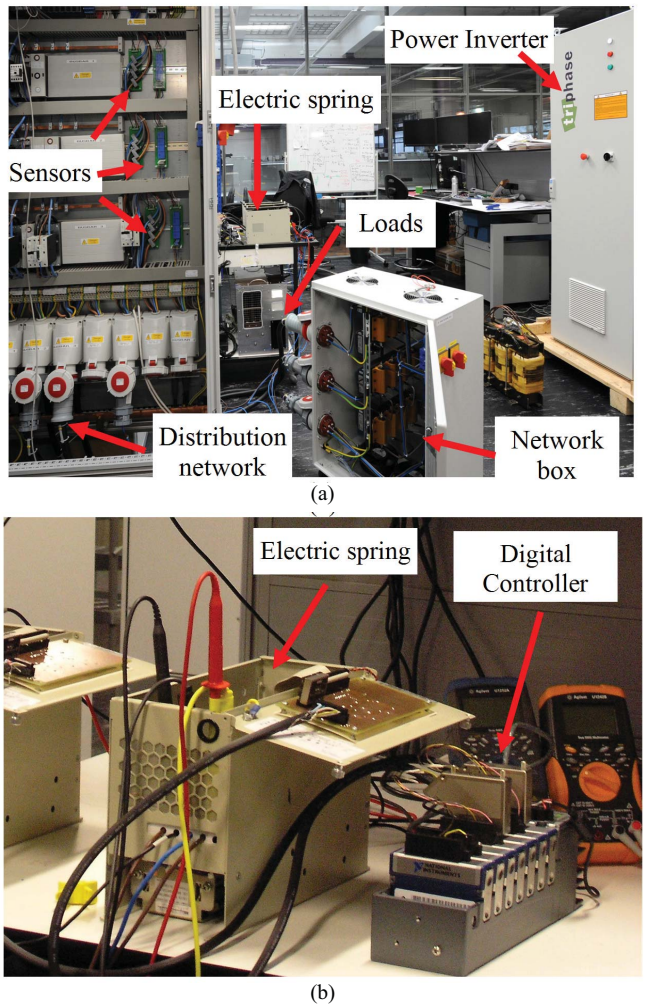

Fig. 9. (a) Photo of the experimental setup in the Maurice Hancock Smart Energy Laboratory at Imperial College London. (b) Photos of the ES prototype and the digital controller.

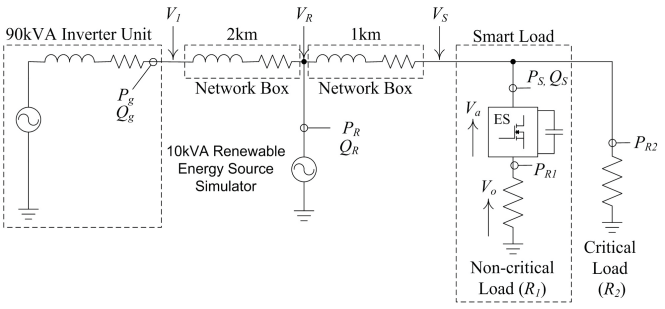

Fig. 10. Schematic of the ES experiment dynamic response measurements.

This paper examines the capability of an ES (connected in series with a noncritical load) in improving voltage stability of a power grid with unstable mains voltage caused by the intermittent renewable power source. The ES, connected in series with a resistive load is programmed specifically to provide reactive power compensation for mains voltage regulation. Two sets of experiments are carried out with different levels of active or reactive power fluctuation generated by the renewable energy source simulator. The simulator is programmed to

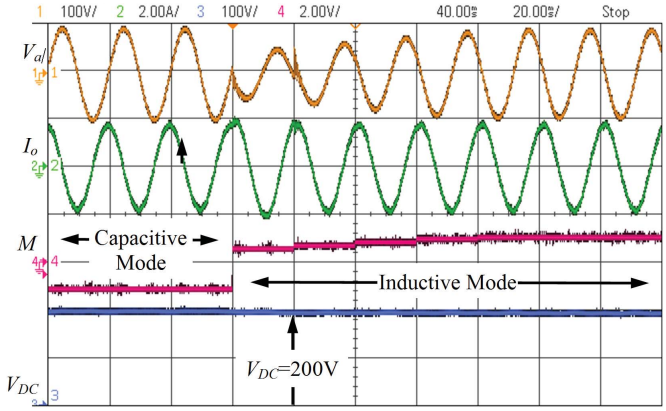

Fig. 11. Step response waveforms of the ac line voltage controller. ES is operating from capacitive to inductive modes. Top to bottom: Ch1, ES voltage V_a 100 V/division (Div); Ch2, noncritical load current I_o 2 A/Div; Ch4, control signal M 2 V/Div; and Ch3, ES dc bus voltage V_{DC} 100 V/Div. Time base 20 ms/Div.

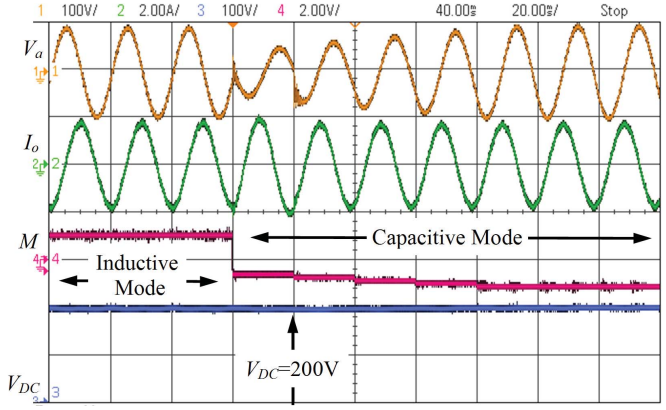

Fig. 12. Step response waveforms of the ac line voltage controller. ES is operating from inductive to capacitive modes. Top to bottom: Ch1, ES voltage V_a 100 V/Div; Ch2, noncritical load current I_o 2 A/Div; Ch4, control signal M 2 V/Div; and Ch3, ES dc bus voltage V_{DC} 100 V/Div. Time base 20 ms/Div.

follow a prerecorded wind power profile that repeats itself in every 360 s. During this experiment, the ES is deactivated in the first pattern (360 s) by closing the mechanical bypass switch. Afterward, it is activated in the second pattern with the bypass switch open. Therefore, the behavior of the power grid with and without ES installation can be observed and compared. The measured mains voltage V_S, noncritical load voltage V_o, ES reactive power Q_S, and noncritical load and critical load power (P_{R1}, P_{R2}) because of the reactive power changes in the power grid are plotted in Figs. 15–17. Similarly, the experimental results of the change of active power generation are shown in Figs. 18–20.

V. Practical Results and Discussion

A. Response of ES Control Loop

Fig. 11 shows the measured step response waveforms of the ES operating from the capacitive mode to the inductive mode. The change of the control signal M (i.e., the inverter modulation index) from -1 to $+1$ signifies the instant of the mode change. For reactive power compensation, the ES generates a compensation voltage V_a that is 90° lagging behind

TABLE III
Detailed System Specifications

System and Loads	
Nominal Phase Voltage (V_l):	220Vac
Non-critical Load Resistance (R_o):	50.5Ω
Other/Critical Load Resistance (R):	53.0Ω
Total Load Power Consumption:	1872W

Network Box		
Distance	Resistance (Ω)	Inductance (mH)
1km	0.1Ω	1.22mH
2km	0.1Ω	2.4mH

90KVA Power Source	
Open Circuit Voltage (E_s):	430V
Short Circuit KVA (SSC):	36KVA
Short Circuit Impedance (Z_s):	5.1
Transformer Reactance Ratio (X/R):	10
Equivalent Output Resistance (R_s):	0.51Ω
Equivalent Output Inductance (L_s):	16.3mH

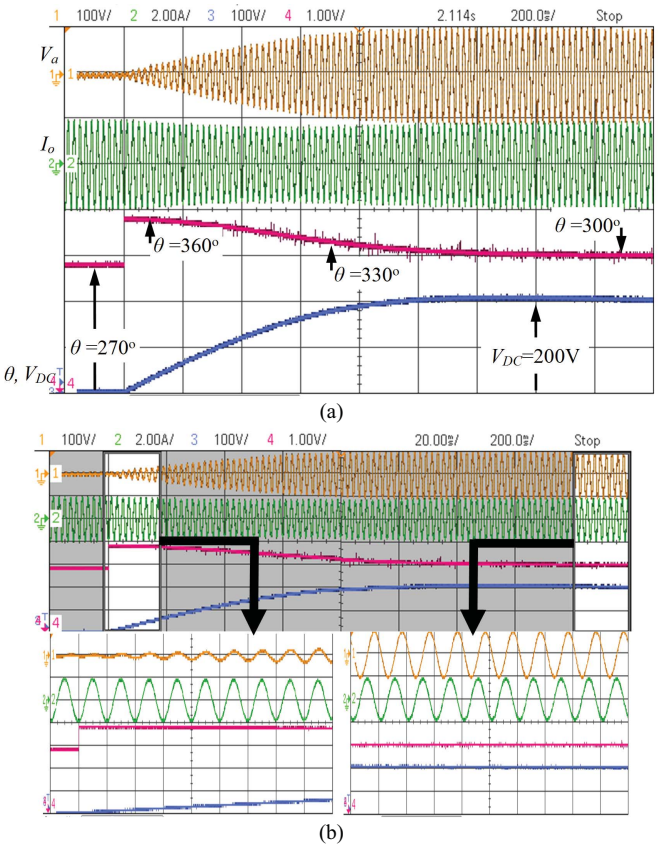

Fig. 13. (a) Transient response waveforms of the dc bus voltage controller. ES is operating in capacitive mode. Top to bottom: Ch1, ES voltage V_a 100 V/Div; Ch2, noncritical load current I_o 2 A/Div; Ch4, control signal θ 100°/Div; and Ch3, ES dc bus voltage V_{DC} 100 V/Div, Time base 200 ms/Div. (b) Enlarged waveforms of (a). Time base 20 ms/Div.

the noncritical load current I_o in the capacitive mode. In the inductive mode, V_a is leading I_o by 90°. The sampling time of the ac line voltage controller is 20 ms. The step response waveforms of ES operating from the inductive mode to the capacitive mode are recorded in Fig. 12. The vectors of V_a and I_o are consistently perpendicular in the reactive power compensation for regulating the mains voltage.

The time responses of the dc bus voltage controller in the capacitive and inductive modes are recorded in Figs. 13 and 14, respectively. When real power is absorbed into the dc

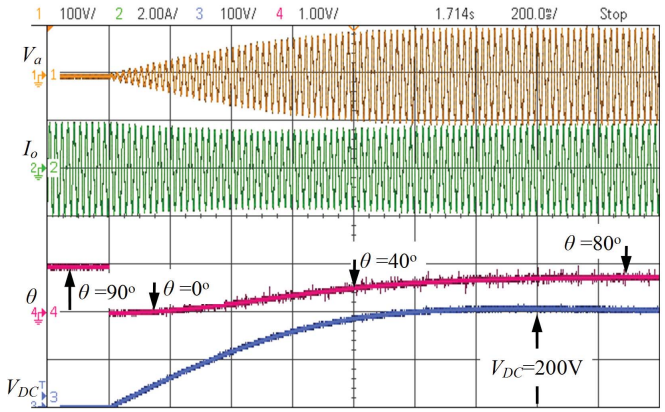

Fig. 14. Transient response of the dc bus voltage controller. ES is operating in the inductive mode. Top to bottom: Ch1, ES voltage V_a 100 V/Div; Ch2, noncritical load current I_o 2 A/Div; Ch4, control signal θ 100°/Div; and Ch3, ES dc bus voltage V_{DC} 100 V/Div. Time base 200 ms/Div.

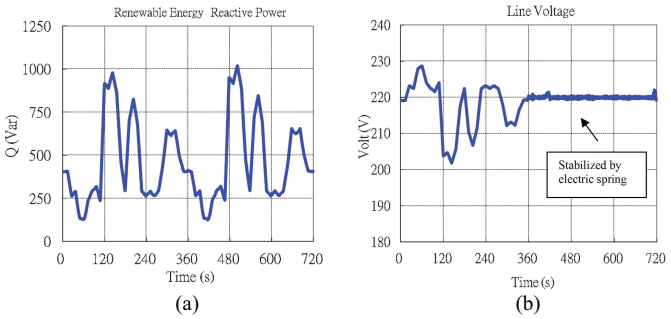

Fig. 15. (a) Prerecorded reactive power profile Q_2 is injected to the power grid using the 10-kVA renewable energy simulator. (b) Measured rms values of the mains voltage V_s before and after the ES is activated. ES is programmed to activate from 360 to 720 s.

capacitor of the power inverter, the vectors of V_a and I_o will deviate from their perpendicular relationship temporarily. This transient behavior can be observed indirectly from the control signal θ, which is also captured to explain the operation. When v_a is zero in the first 200 ms of Fig. 13(a), the initial θ is 270° in the capacitive mode. When v_a is zero, V_s and I_o are in phase for the pure resistive noncritical load. As θ is the angle between V_s and V_a, the vectors of V_a and I_o are perpendicular. After the initial 200 ms, the ES comes into action. The dc bus is increased (by transferring energy into the dc capacitor) for providing the ES voltage v_a. It can be seen that θ now deviates from its initial value of 270° to 360° and then gradually settles down to ~300°. The steady value of θ in Fig. 13(a) is not 270° because the ES acting as an equivalent capacitor in series with the resistive noncritical load will change the angle between V_s and I_o. V_s and I_o are no longer in phase because of the presence of the equivalent capacitive of the ES working in the capacitive mode. The enlarged waveforms at the initial state and steady state of the step response in Fig. 13(a) are shown in Fig. 13(b). In the initial state, the spring voltage and current are in phase as real power is being transferred to charge the dc capacitor. Under steady-state condition (when the dc capacitor is fully charged to 200 V), V_a lags behind I_o by 90° and the function of the ES for reactive power compensation continues.

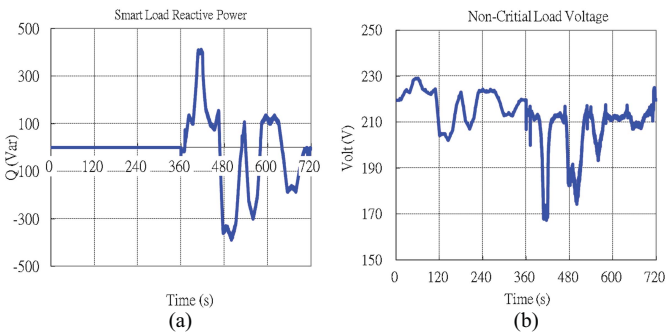

Fig. 16. Measured (a) reactive power of the smart load Q_s and (b) rms values of the noncritical load voltage V_o before and after the ES is activated. A repeated reactive power profile of 360 s is fed to the power grid [see Fig. 9(a)]. ES is programmed to activate from 360 to 720 s.

The step response test of the dc bus controller is repeated with the ES working in the inductive mode. Similar behaviors can be observed in Fig. 14. Again, the ES is activated after the first 200 ms. The angle θ deviates from 90° to 0° when real power is absorbed to charge up the dc capacitor. The angle settles at 80° under steady-state conduction. V_a leads I_o by 90° during the steady-state condition when the ES operates under the inductive mode.

B. Response of ES to the Reactive Power Changes

In the first experiment, a prerecorded reactive power profile is fed to the renewable energy source simulator to generate a weakly regulated ac mains voltage at the power line repeatedly [see Fig. 15(a)]. The bypass switch is closed in the first pattern (first 360 s) and then opened in the second pattern to allow the ES to take actions. Fig. 15(b) shows the measured rms value of the mains voltage V_s before and after the ES is activated. From the first pattern of Fig. 15(b), because of the changes of the reactive power along the distribution network, the mains voltage is fluctuating between 227 and 205 Vac. With the bypass switch opened at 360 s, the ES is activated when the pattern is repeated. The mains voltage V_s can be regulated at the nominal voltage of 220 Vac.

The smart load reactive power and the voltage across the noncritical load are shown in Fig. 16(a) and (b), respectively. The ES reduces the voltage of the noncritical load V_o and generates reactive power Q_s to the power system simultaneously. With the observation of the measured mains voltage and smart-load reactive power data, the ES generates positive (inductive) reactive power to suppress the mains voltage. If voltage support is required, the ES generates negative (capacitive) reactive power to the power grid. Therefore, the noncritical load power P_{R1} is automatically adjusted and the critical load power P_{R2} is kept constant, as shown in Fig. 17(a) and (b), respectively. These results confirm the successful operations of the input voltage control mechanism and the voltage regulation capability of the ES.

C. Response of ES to the Active Power Changes

To further examine the effectiveness of the ES in a power grid with high-penetration intermittent wind energy, the

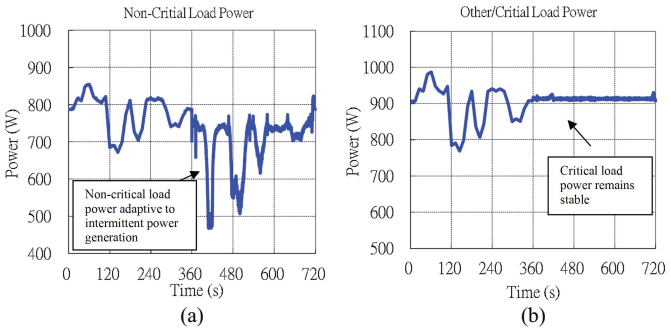

Fig. 17. Measured (a) noncritical load power P_{R1} and (b) critical load power P_{R2} before and after the ES is activated. A repeated reactive power profile of 360 s is fed to the power grid [see Fig. 9(a)]. ES is programmed to activate from 360 to 720 s.

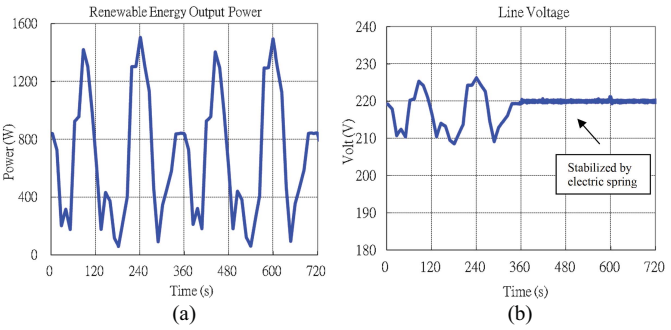

Fig. 18. (a) Prerecorded active power profile P_2 injected to the power grid using the 10-kVA renewable energy simulator. (b) Measured rms values of the mains voltage V_s before and after the ES is activated. ES is programmed to activate from 360 to 720 s.

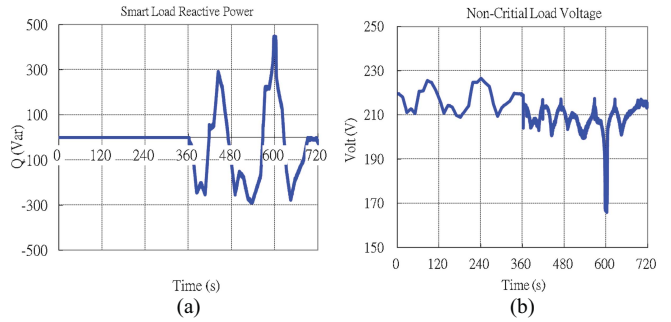

Fig. 19. Measured (a) reactive power of the smart load Q_s and (b) rms values of the noncritical load voltage V_o before and after the ES is activated. A repeated active power profile of 360 s is fed to the power grid [see Fig. 12(a)]. ES is programmed to activate from 360 to 720 s.

renewable energy source simulator is programmed to simulate a dynamically fluctuating wind power generator. Fig. 18(a) shows the prerecorded wind power profile of 360 s. Note that the maximum wind power is 1500 W. The penetration is up to 80% of the total load power demand (1872 W). Therefore, the electric power from the traditional power substation is only a small portion of total load demand. Because of the stochastic nature of wind speed, the output power, however, can be dramatically dropped to a very low value. Without energy storage system installed in the power grid, the high dynamic changes of wind power lead to instability in the power grid. In Fig. 18(b), the mains voltage V_S is fluctuating

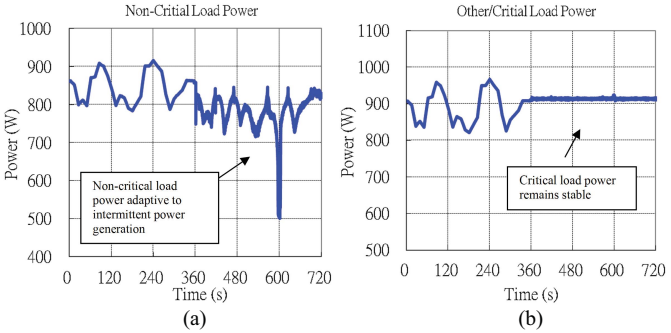

Fig. 20. Measured (a) noncritical load power P_{R1} and (b) critical load power P_{R2} before and after the ES is activated. A repeated reactive power profile of 360 s is fed to the power grid [see Fig. 12(a)]. ES is programmed to activate from 360 to 720 s.

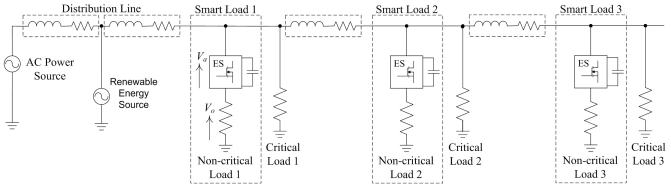

Fig. 21. Typical distributed implementation of ESs in distribution network.

in the region above and below the rated value of 220 Vac in the first half of the test when the ES is not in action.

Same as the previous test, the profile is repeated after 360 s and ES is activated. From the period of 360–720 s, the ES generates positive or negative reactive power to the power grid to regulate the mains voltage at 220 Vac successfully. In Fig. 19(a) and (b), the noncritical load voltage is reduced and the reactive power generated from the ES is following the mains voltage fluctuation. The noncritical and critical load power profiles are measured and shown in Fig. 20(a) and (b), respectively. The critical load power remains essentially the same. These results confirm the effectiveness of using ES to improve power system stability with high penetration of intermittent renewable energy source.

D. On the Reactive Power (kVA) Rating

In this experimental prototype (for demonstration purpose), the kVA rating is ~0.58 kVA. The kVA rating of an ES is the product of the variable voltage range of the ES and the rated current of the series-connected load. In this implementation example, the ES voltage range (Table I) is arbitrarily chosen at 134 V and the noncritical load current is 4.36 A (i.e., 220 V/50.5 Ω). The noncritical load voltage can be reduced to ~170 V, as shown in Fig. 19(b). The reactive power rating of an ES, however, could be much smaller in practice. ESs are supposed to be embedded in a new generation of smart loads that are adaptive to substantial mains voltage fluctuations. Examples of such smart loads include electric water heaters, refrigerators, and some public lighting systems. These types of smart loads (and their embedded ESs) will be distributed over the distribution power network as shown in Fig. 21. If the noncritical load voltage is to be reduced to not <200 V, for the same experimental setup, the ES voltage variation is reduced

to ~90 V, indicating that the kVA rating will be reduced from 0.58 to ~0.39 kVA. Although individual ESs could have small kVA ratings, it is the collective efforts of many distributed ESs that would provide the distributed voltage support for the power grid.

VI. Conclusion

This paper describes the hardware and control implementation of an ES to form a smart load unit. The control method for the ES for reactive power compensation and mains voltage regulation was proposed and realized by a digital controller. The performance of the ES was analyzed and practically evaluated in a 90-kVA electric power grid. The voltage fluctuation of the power grid was created by a 10-kVA renewable energy source simulator. A prerecorded power profile was programmed into the simulator to create a weakly regulated power grid. It is found that the ES can automatically perform voltage support, suppression, and load-shedding functions in response to the dynamic needs of the power grid. It is envisaged that ES can be a useful apparatus for the stability control of future smart grid with substantial penetration of intermittent renewable energy sources. The significance of this ES-based stability control lies in the fact that these ESs can be distributed all over the power grid for decentralized stability control without any dependence on ITC, smart metering, and wide-area power management. It is a new methodology that can turn many noncritical loads into a new generation of smart loads that have their load demands automatically following power generation—which is the new control paradigm required by future power grid with distributed renewable power sources. The next stage of our research will include cost and performance comparison of ESs with other real-time demand-side management methods.

Acknowledgment

The authors would like to thank the Maurice Hancock Smart Energy Laboratory of Imperial College, London, U.K., for providing the facilities for testing the ESs.

References

[1] *China Eye s 20% Renewable Energy By 2020*, China Daily News, Taiwan, China, Jun. 2009.

[2] *On Investing in the Development of Low Carbon Technologies (SET-Plan)*, Commission of European Communities, Brussels, Belgium, Oct. 2009.

[3] (2008, Jan.). *Proposal for a Directive of the European Parliament and of the Council on the Promotion of the use of Energy from Renewable Sources* [Online]. Available: http://eur-lex.europa.eu/LexUriServ/LexUriServ.do?uri=COM:2008:0019:FIN:EN:PDF

[4] D. Westermann and A. John, "Demand matching wind power generation with wide-area measurement and demand-side management," *IEEE Trans. Energy Convers.*, vol. 22, no. 1, pp. 145–149, Mar. 2007.

[5] P. Palensky and D. Dietrich, "Demand side management: Demand response, intelligent energy systems, and smart loads," *IEEE Trans. Ind. Informat.*, vol. 7, no. 3, pp. 381–388, Aug. 2011.

[6] I. Koutsopoulos and L. Tassiulas, "Challenges in demand load control for the smart grid," *IEEE Netw.*, vol. 25, no. 5, pp. 16–21, Sep.–Oct. 2011.

[7] A. Mohsenian-Rad, V. W. S. Wong, J. Jatskevich, R. Schober, and A. Leon-Garcia, "Autonomous demand-side management based on game-theoretic energy consumption scheduling for the future smart grid," *IEEE Trans. Smart Grid*, vol. 1, no. 3, pp. 320–331, Dec. 2010.

[8] M. Parvania and M. Fotuhi-Firuzabad, "Demand response scheduling by stochastic SCUC," *IEEE Trans. Smart Grid*, vol. 1, no. 1, pp. 89–98, Jun. 2010.

[9] M. Pedrasa, T. D. Spooner, and I. F. MacGill, "Scheduling of demand side resources using binary particle swarm optimization," *IEEE Trans. Power Syst.*, vol. 24, no. 3, pp. 1173–1181, Mar. 2009.

[10] F. Kienzle, P. Ahčin, and G. Andersson, "Valuing investments in multi-energy conversion, storage, and demand-side management systems under uncertainty," *IEEE Trans. Sustain. Energy*, vol. 2, no. 2, pp. 194–202, Feb. 2011.

[11] A. J. Conejo, J. M. Morales, and L. Baringo, "Real-time demand response model," *IEEE Trans. Smart Grid*, vol. 1, no. 3, pp. 236–242, Dec. 2010.

[12] A.-H. Mohsenian-Rad and A. Leon-Garcia, "Optimal residential load control with price prediction in real-time electricity pricing environments," *IEEE Trans. Smart Grid*, vol. 1, no. 2, pp. 120–133, Sep. 2010.

[13] A. J. Roscoe and G. Ault, "Supporting high penetrations of renewable generation via implementation of real-time electricity pricing and demand response," *IET Renew. Power Generat.*, vol. 4, no. 4, pp. 369–382, Jul. 2010.

[14] S. C. Lee, S. J. Kim, and S. H. Kim, "Demand side management with air conditioner loads based on the queuing system model," *IEEE Trans. Power Syst.*, vol. 26, no. 2, pp. 661–668, May 2011.

[15] G. C. Heffner, C. A. Goldman, and M. M. Moezzi, "Innovative approaches to verifying demand response of water heater load control," *IEEE Trans. Power Del.*, vol. 21, no. 1, pp. 388–397, Jan. 2006.

[16] A. Brooks, E. Lu, D. Reicher, C. Spirakis, and B. Weihl, "Demand dispatch," *IEEE Power Energy Mag.*, vol. 8, no. 3, pp. 20–29, Jun. 2010.

[17] S. Y. R. Hui, C. K. Lee, and F. F. Wu, "Power control circuit and method for stabilizing a Power Supply," U.S. Patent 61 389 489, Oct. 4, 2010.

[18] (2009, Nov.). *Hooke's Law—Britannica Online Encyclopedia* [Online]. Available: http://www.britannica.com/EBchecked/topic/271336/Hookes-law

[19] J. Dixon L. Moran, J. Rodriguez, R. Domke, "Reactive power compensation technologies: State-of-the-art review," *Proc. IEEE*, vol. 93, no. 12, pp. 2144–2164, Dec. 2005.

[20] H. K. Tyll and F. Schettle, "Historical overview on dynamic reactive power compensation solutions from the begin of AC power transmission towards present applications," in *Proc. IEEE Power Syst. Conf. Exposit.*, Mar. 2009, pp. 1–7.

[21] P. Sauer, "Reactive power and voltage control issues in electric power systems," in *Proc. Appl. Math. Res. Electr. Power Syst. Conf.*, Apr. 2005, pp. 11–24.

[22] J. Li, J. Liu, D. Boroyevich, P. Mattavelli, and Y. Xue, "Three-level active neutral-point-clamped zero-current-transition converter for sustainable energy systems," *IEEE Trans. Power Electron.*, vol. 26, no. 12, pp. 3680–3693, Dec. 2011.

[23] R. I. Bojoi, L. R. Limongi, D. Roiu, and A. Tenconi, "Enhanced power quality control strategy for single-phase inverters in distributed generation systems," *IEEE Trans. Power Electron.*, vol. 26, no. 3, pp. 798–806, Mar. 2011.

[24] N. Mohan, T. Undeland, and W. Robbins, *Power Electronics: Converters, Applications and Designs*, 2nd ed. New York, NY, USA: Wiley, 1995, pp. 691–693.

[25] S. Y. R. Hui, C. K. Lee, and F. Wu, "Electric springs—A new smart grid technology," *IEEE Trans. Smart Grid*, vol. 3, no. 3, Sep. 2012, pp. 1552–1561.

[26] S. C. Tan, C. K. Lee, and S. Y. R. Hui, "General steady-state analysis and control principle of electric springs with active and reactive power compensations," *IEEE Trans. Power Electron.*, vol. 28, no. 8, pp. 3958–3969, Aug. 2013.

[27] C. K. Lee and S. Y. R. Hui, "Reduction of energy storage requirements for smart grid using electric springs," *IEEE Trans. Smart Grid*, (early access).

Chi Kwan Lee (M'08) received the B.Eng. and Ph.D. degrees in electronic engineering from the City University of Hong Kong, Kowloon, Hong Kong, in 1999 and 2004, respectively.

He was a Post-Doctoral Research Fellow with the Power and Energy Research Center, National University of Ireland, Galway, Ireland, from 2004 to 2005. In 2006, he joined the Center of Power Electronics, City University of Hong Kong, as a Research Fellow. From 2008 to 2011, he was a Lecturer of electrical engineering with Hong Kong Polytechnic University, Hong Kong. He was a Visiting Academic with Imperial College London, London, U.K., from 2010 to 2012. Since January 2012, he has been an Assistant Professor with the Department of Electrical and Electronic Engineering, University of Hong Kong, Hong Kong. He is a co-inventor of the electric springs and a planar EMI filter. His current research interests include applications of power electronics to power systems, advanced inverters for renewable energy and smart grid applications, reactive power control for load management in renewable energy systems, wireless power transfer, energy harvesting, and planar electromagnetics for high frequency power converters.

Balarko Chaudhuri (M'06–SM'11) received the Ph.D. degree from Imperial College London, London, U.K., in 2005.

He is currently a Senior Lecturer with the Control and Power Research Group, Imperial College London. His current research interests include electric power transmission systems, control theory, smart grids, and renewable energy.

Dr. Chaudhuri a Member of the IET and Cigre. He is an Associate Editor of the IEEE SYSTEMS JOURNAL and *Elsevier Control Engineering Practice*.

Shu Yuen Hui (M'87–SM'94–F'03) received the B.Sc. degree in engineering (Hons.) from the University of Birmingham, Birmingham, U.K., in 1984, and the D.I.C. and Ph.D. degrees from the Imperial College London, London, U.K., in 1987.

He has previously held academic positions with the University of Nottingham, Nottingham, U.K., from 1987 to 190, University of Technology, Sydney, Australia, from 1990 to 1991, University of Sydney, Sydney, from 1992 to 1996, and City University of Hong Kong, Hong Kong, from 1996 to 2011. Currently, he is the Philip Wong Wilson Wong Chair Professorship with the University of Hong Kong, Hong Kong. Since July 2010, he has concurrently held the Chair Professorship of Power Electronics with Imperial College London. He has published over 270 technical papers, including more than 160 refereed journal publications and book chapters. His patents have been adopted by industry.

Dr. Hui is a Fellow of IET. He has been an Associate Editor of the IEEE TRANSACTIONS ON POWER ELECTRONICS since 1997 and an Associate Editor of the IEEE TRANSACTIONS ON INDUSTRIAL ELECTRONICS since 2007. He has been appointed twice as an IEEE Distinguished Lecturer by the IEEE Power Electronics Society in 2004 and 2006. He served as one of the 18 Administrative Committee members of the IEEE Power Electronics Society and was the Chairman of its Constitution and Bylaws Committee from 2002 to 2010. He was a recipient of the Teaching Excellence Award in 1998 and the Earth Champion Award in 2008. He was a recipient of the IEEE Best Paper Award from the IEEE IAS Committee on Production and Applications of Light in 2002, and two IEEE Power Electronics Transactions Prize Paper Awards for his publications on Wireless Charging Platform Technology in 2009 and on LED System Theory in 2010. His inventions on wireless charging platform technology underpin key dimensions of Qi, the world's first wireless power standard, with freedom of positioning and localized charging features for wireless charging of consumer electronics. He is a co-inventor of electric springs. In 2010, he was a recipient of the IEEE Rudolf Chope R&D Award from the IEEE Industrial Electronics Society, the IET Achievement Medal (The Crompton Medal), and he was elected to the Fellowship of the Australian Academy of Technological Sciences and Engineering.